*The Canadian Mineralogist*
Vol. 35, pp. 1051-1067 (1997)

# TECTONOMETAMORPHIC EVOLUTION OF THE SOUTHERN TALTSON MAGMATIC ZONE AND ASSOCIATED SHEAR ZONES, NORTHEASTERN ALBERTA[1]

TIMOTHY W. GROVER* and DAVID R.M. PATTISON

*Department of Geology and Geophysics, University of Calgary, Calgary, Alberta T2N 1N4*

MICHAEL R. McDONOUGH

*Geological Survey of Canada, 3303 33rd Street NW, Calgary, Alberta T2N 2N7*

VICKI J. McNICOLL

*Geological Survey of Canada, 601 Booth Street, Ottawa, Ontario K1A 0E8*

## Abstract

The petrology of pelitic paragneisses provides constraints on the tectonometamorphic evolution of the Paleoproterozoic southern Taltson Magmatic Zone (TMZ) and associated north-trending shear zones, exposed in northeastern Alberta. Paragneiss bodies within the TMZ occur as discontinuous, elongate, north-trending lenses and schlieren, ranging in size from <1 m to >10 km in length, in associated plutonic rocks and basement gneisses. Four distinct assemblages of metamorphic minerals are recognized within the metapelitic gneisses. From west to east across the area, these assemblages are: 1) Spl + Qtz + Grt + Crd + Kfs + Sil, 2) Spl +Qtz + Bt + Grt + Crd + Kfs + Sil, 3) Grt + Bt + Crd + Kfs + Sil + Qtz with Spl inclusions in Grt and Crd, and 4) Grt + Bt + Crd + Kfs + Sil + Qtz. The mineral assemblages suggest a range in metamorphic grade from upper granulite to lower granulite facies. Migmatites are associated with the metapelitic gneisses throughout the area. The stable association of Spl + Qtz assemblages, dependent on the effects of minor components in spinel and garnet, requires metamorphic temperatures in excess of 850°C. The results of geothermobarometric calculations vary widely, but maximum calculated temperatures exceed 850°C. Calculated metamorphic pressures are approximately 5–7 kbars. Ductile deformation of the assemblage Grt + Crd + Kfs + Sil + Qtz ± Spl in the north-trending Leland Lake and Charles Lake shear zones suggests deformation initiated under granulite-facies conditions. Successive overprinting of granulite-grade assemblages by amphibolite- and greenschist-grade assemblages demonstrates that shear-zone movement took place during cooling and hydration of the southern TMZ.

*Keywords*: granulite, mylonite, spinel + quartz, Taltson Magmatic Zone, Alberta basement.

## Sommaire

Une étude pétrologique de paragneiss pélitiques vient préciser l'évolution tectonométamorphique du secteur sud de la zone magmatique de Taltson, d'âge paléoprotérozoïque, qui affleure dans le coin nord-est de l'Alberta, associée à des zones de cisaillement orientées vers le nord. Les massifs paragneissiques sont des lentilles et des schlieren allongés vers le nord, discontinus, allant de <1 m à >10 km en longueur, associés à des roches plutoniques et des gneiss du socle. Nous distinguons quatre assemblages de minéraux métamorphiques dans ces gneiss métapélitiques. D'ouest en est, ils sont: 1) Spl + Qtz + Grt + Crd + Kfs + Sil, 2) Spl + Qtz + Bt + Grt + Crd + Kfs + Sil, 3) Grt + Bt + Crd + Kfs + Sil + Qtz avec inclusions de Spl dans le grenat et la cordiérite, et 4) Grt + Bt + Crd + Kfs + Sil + Qtz. Ces assemblages témoignent d'un intervalle d'intensité de métamorphisme allant du faciès granulite supérieur à inférieur. Des migmatites sont associées aux gneiss métapélitiques dans toute la région. L'association stable de spinelle + quartz, compte tenu de l'influence de composants mineurs dans le spinelle et le grenat, implique une température de métamorphisme dépassant 850°C. Les résultats de calculs géothermobarométriques sont très variables, mais les températures maximales dépassent 850°C. L'intervalle de pressions calculées est environ 5–7 kbars. La déformation ductile de l'assemblage Grt + Crd + Kfs + Sil + Qtz ± Spl dans les zones de cisaillement nord–sud de Leland Lake et Charles Lake fait penser qu'elle a débuté à des conditions typiques du faciès granulite. Des épisodes de recristallisation successives ont transformé les assemblages du faciès granulite à des assemblages typiques des faciès amphibolite et schistes verts; selon ces ajustements, le mouvement le long des zones de cisaillement aurait eu lieu pendant le refroidissement et l'hydratation du secteur sud de la zone magmatique de Taltson.

(Traduit par la Rédaction)

*Mots-clés*: granulite, mylonite, spinelle + quartz, zone magmatique de Taltson, socle de l'Alberta.

[1] LITHOPROBE publication number 876.

* Present address: Department of Natural Sciences, Castleton State College, Castleton, Vermont 05735, U.S.A.
*E-mail address*: grovert@sparrow.csc.vsc.edu

## Introduction

The Precambrian rocks of the Canadian Shield exposed in the northeastern corner of Alberta (Fig. 1) are the only exposure in Alberta of basement rocks east of the Rocky Mountains. Understanding the geological evolution of these rocks through detailed field-based studies where relationships are readily exposed at the surface, provides a framework or "ground truth" for studies of the subsurface basement elsewhere in Alberta (Ross *et al.* 1991, Thériault & Ross 1991, Villeneuve *et al.* 1993). Recent geophysical and geochronological studies of the Alberta basement have shown that it is a mosaic of different domains distinguished on the basis of distinctive aeromagnetic and gravity signatures, and age ranges determined from single-crystal zircon U–Pb studies (Ross *et al.* 1991, Villeneuve *et al.* 1993). In addition, the rocks in northeastern Alberta form the southern extension of the Taltson Magmatic zone, part of a continent-scale magmatic arc which is located between two large-scale shear zones: the Great Slave Lake Shear Zone and the Snowbird Tectonic Zone (Fig. 1). Understanding the geological evolution of this region is important to constrain models of the tectonic assembly of western Laurentia.

This study concentrates on deciphering the tectonic-thermal evolution of the crust in northeastern Alberta by studying the petrology of metapelitic rocks that occur as discontinuous bodies throughout the study area. Field relationships, petrographic relationships, consideration of phase diagrams, and geothermobarometry are used to constrain the P–T state of the crust during regional high-grade metamorphism and magmatism, and subsequent development of north-trending shear zones that dissect the study area.

### *Regional tectonic setting*

The study area lies largely within the southern Taltson Magmatic Zone (TMZ), south of the Great Slave Lake Shear Zone (GSLSZ) and north of the Snowbird Tectonic Zone (STZ) (Fig. 1). The rocks in northeastern Alberta represent the southernmost exposure of the Taltson–Thelon magmatic arc. The Taltson–Thelon magmatic arc formed during the convergence and collision of the Archean Rae and Slave provinces to the north of the GSLSZ and the Slave province and the Buffalo Head terrane south of the GSLSZ (Hoffman 1988, Ross *et al.* 1991).

The Buffalo Head terrane and the Rae Province are chronologically distinct. The Buffalo Head terrane, which is not exposed at the surface, has been characterized entirely on the basis of geophysical studies and isotopic analysis of core samples (Ross *et al.* 1991, Thériault & Ross 1991). The Buffalo Head terrane is composite, consisting largely of granitic rocks considered to represent the roots of a series of accreted volcanic arcs. U–Pb ages determined from single-crystal studies of zircon and monazite from drill-core samples reveal that rocks from the Buffalo Head terrane range in age from approximately 2.4 to 2.1 Ga (Ross *et al.* 1991). These ages are significantly younger than the 2.4 Ga and older ages that characterize the basement of the western portion of the Rae Province in this region (van Breemen *et al.* 1992), but older than the rocks of the southern TMZ (see discussion to follow; McDonough *et al.* 1997).

The TMZ is interpreted as a composite Andean-type and continent-collision orogen formed in response to the collision and accretion of the Buffalo Head Terrane to the Rae Province (Fig. 1; Ross *et al.* 1991, Ross *et al.* 1995). Isotopic and geochemical data, largely derived from rocks from the northern TMZ, suggest that the TMZ is a magmatic belt consisting of precollisional, I-type, volcanic-arc-related magmatic rocks and postcollisional, anatectically generated S-type batholiths (Hoffman 1988, Ross *et al.* 1991, Thériault 1992). However, this interpretation is not universally accepted. A recent Nd, Pb, and O isotopic study on southern TMZ granitic rocks indicates that the isotope systematics of what were interpreted to be I-type plutons can be accounted for by melting of crustal source-rocks with little to no mantle involvement (De *et al.* 1997). U–Pb single grain studies on zircon and monazite from granitic rocks from the southern TMZ reveal crystallization ages between 2.0 and 1.8 Ga (McDonough *et al.* 1997). The area is cut by several north-trending shear zones, thought to be generated by the southward movement of crustal blocks in response to indentation of the Rae Province by the Slave Province and movement along the GSLSZ (Hanmer *et al.* 1992a, b). Although aeromagnetic studies suggest that the shear zones are truncated by the STZ to the south, the geological relationship between north-trending shear zones and the STZ is enigmatic. The STZ is considered to be an Archean structure to the northeast where it has been studied at the surface (Hanmer *et al.* 1992a), whereas the north-trending shear zones are of Proterozoic age (McDonough *et al.* 1997).

## General Geology of the Southern Taltson Magmatic Zone

The Canadian Shield in northeastern Alberta was studied and mapped by Godfrey and others from the late 1950s through the early 1970s [see Godfrey (1986) and references contained therein]. Recent investigations in the area, supported by a joint GSC – Alberta MDA project, resulted in a new series of 1:50,000 scale, digitally based geological maps [McDonough *et al.* (1997), and references contained therein]. A generalized compilation of this recent mapping is shown in Figure 2.

The area is predominantly underlain by numerous granitic plutons including: the Slave granite, a weakly

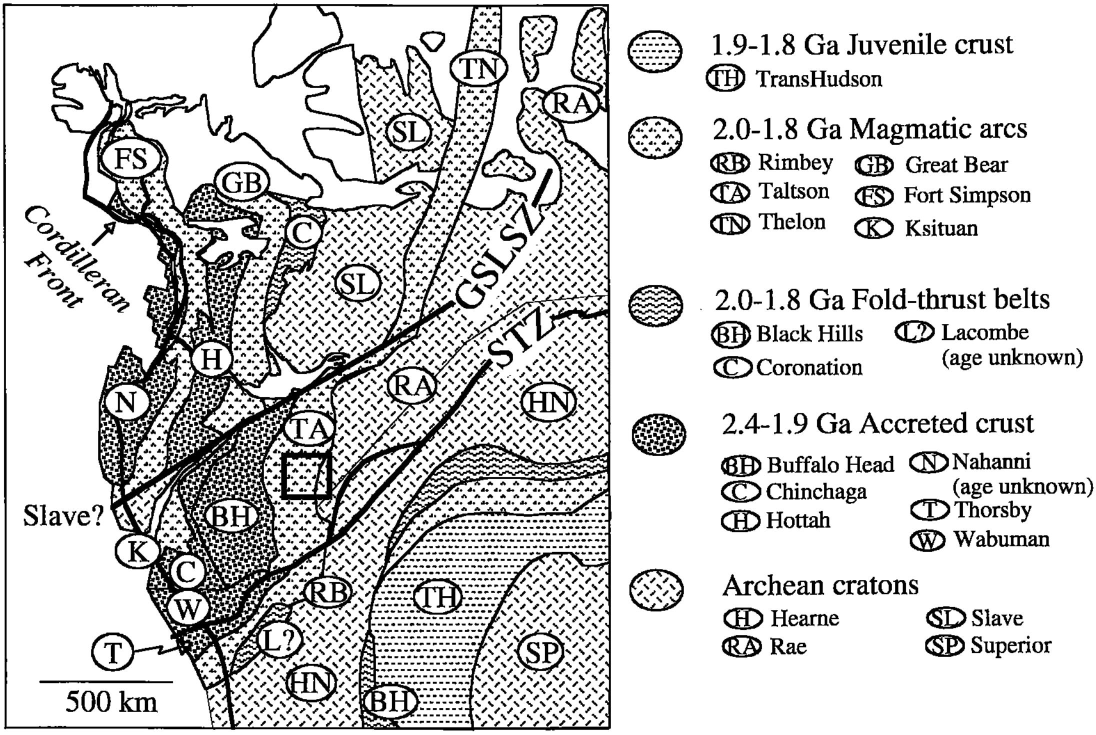


FIG. 1. Generalized geological map of western Laurentia, after Hoffman (1988) and Ross *et al.* (1991). The map area corresponds to the square. GSLSZ and STZ designate the Great Slave Lake Shear Zone and the Snowbird Tectonic Zone, respectively.

foliated S-type granite with abundant biotite – garnet – cordierite – hercynite clots and inclusions of anhydrous, restitic, pelitic gneiss (Fig. 3a; Chacko *et al.* 1994, Chacko & Creaser 1995, Chacko 1997), the Chipewyan granite, a medium-grained, magnetite-bearing, pink to red granite, the Charles Lake granite, a foliated, K-feldspar megacrystic biotite-bearing granite, the Arch Lake granite, a strongly deformed K-feldspar granitic to syenogranitic gneiss, the Wylie Lake granodiorite, another strongly deformed, K-feldspar megacrystic, biotite–hornblende granodioritic gneiss, the Colin Lake muscovite granite, a weakly foliated, muscovite-bearing white granite, and the Andrew Lake granodiorite, a well-foliated, biotite–hornblende granodiorite (McDonough *et al.* 1997). Field relationships show that the plutonic rocks, with ages of crystallization ranging from approximately 1.99 to 1.92 Ga, were emplaced before, during, and after movement along several north-trending shear zones (McDonough *et al.* 1997).

The Taltson basement complex (TBC) represents the basement into which many of the plutonic rocks were emplaced. The TBC, although lithologically heterogeneous, is predominantly a banded, pink, biotite- or hornblende-bearing granitic gneiss. These rocks have a bimodal distribution of ages, ranging from 3.2 to 2.9 Ga and from 2.4 to 2.0 Ga, which suggests that they may be fragments of either the Buffalo Head or Rae Province cratons (Ross *et al.* 1991, Villeneuve *et al.* 1993).

The metasedimentary rocks, although volumetrically subordinate, are present throughout the area (Fig. 2), and are the focus of this study. The metasedimentary rocks are primarily pelitic, semi-pelitic, and psammitic paragneisses, with subordinate amounts of calc-silicates and quartzites. These rocks have been correlated with those of the Rutledge River basin found in the northern TMZ (Bostock & van Breemen 1994, McDonough *et al.* 1997). The metasedimentary rocks occur as irregularly shaped lenses forming discontinuous elongate bodies, ranging in length from less than a meter to greater than 10 kilometers, as schlieren within granitic gneisses, and as centimeter- to meter-scale inclusions in granitic rocks. The long axes of the mappable metasedimentary bodies are generally parallel to the northerly trend of the shear zones (Fig. 2), and the paragneiss invariably has a prominent foliation that is locally mylonitic.

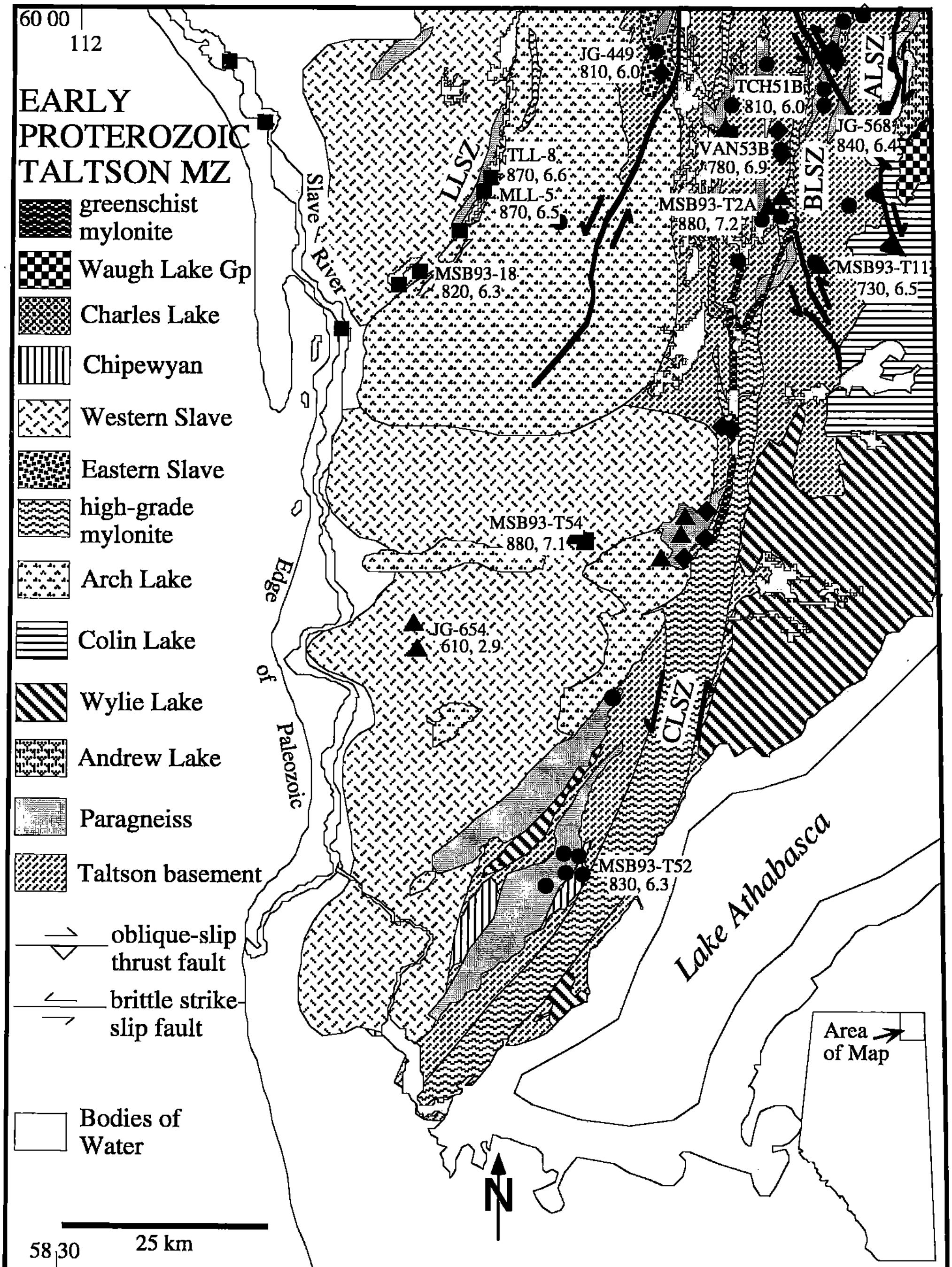


FIG. 2. Generalized geological map of the southern Taltson Magmatic Zone, after McDonough *et al.* (1997), and assemblage map showing the distribution of assemblages of high-grade metamorphic minerals. LLSZ, CLSZ, BLSZ, and ALSZ designate the Leland Lake, Charles Lake, Bayonet Lake and Andrew Lake shear zones, respectively. Mineral assemblages as follows: squares: Spl + Qtz + Grt + Crd + Kfs + Sil; triangles: Spl + Qtz + Bt + Grt + Crd + Kfs + Sil; circles: Grt + Bt + Crd + Kfs + Sil + Qtz, with Spl inclusions in Grt and Crd; diamonds: Grt + Bt + Crd + Kfs + Sil + Qtz. P–T estimates are taken from Table 6 and are discussed in the text. The temperature estimates are based on the Grt–Crd Fe–Mg exchange equilibrium.

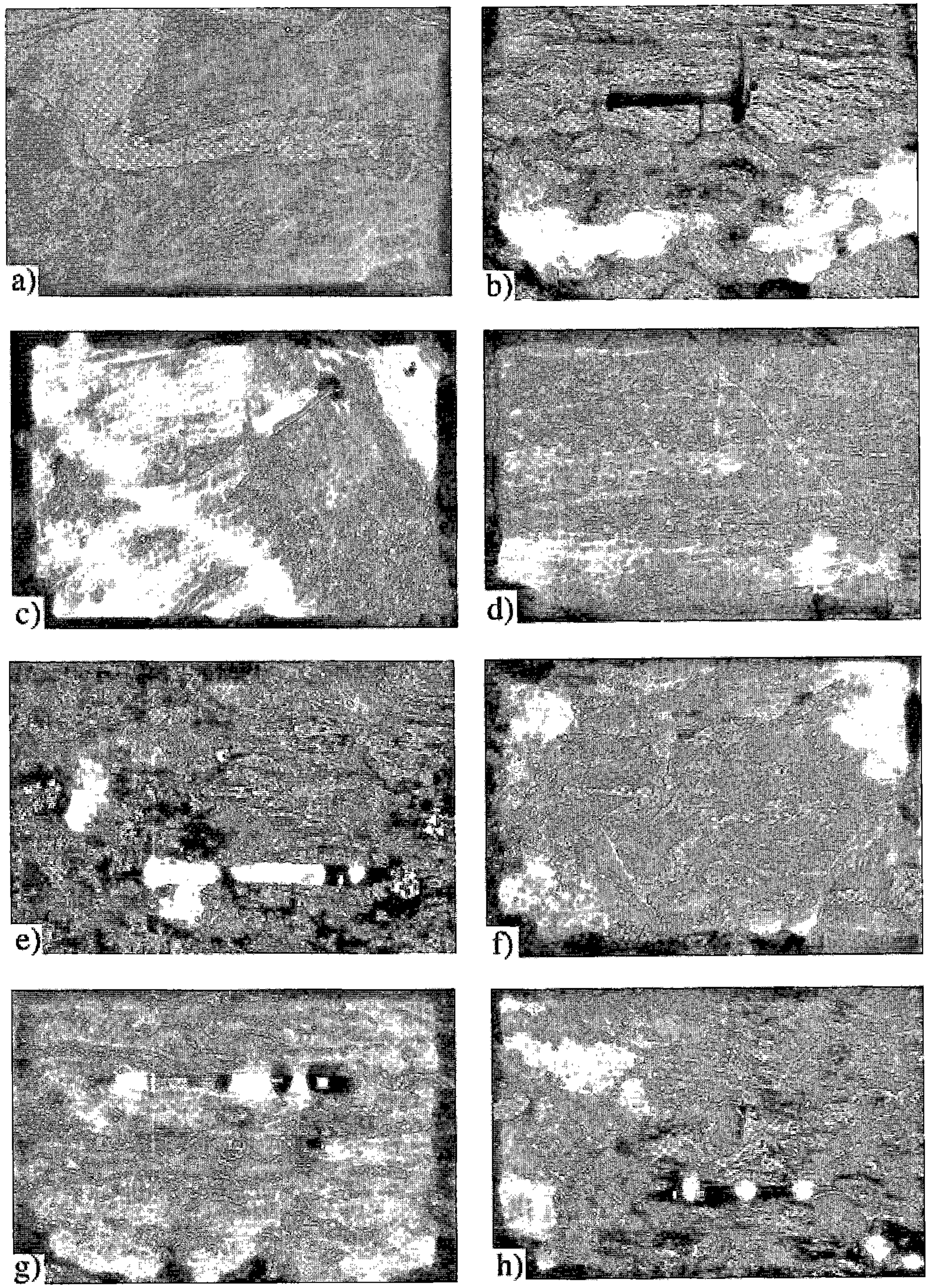


FIG. 3. Field photographs of metasedimentary rocks. a. A block of restitic paragneiss in Slave granite from Pelican Rapids along the Smith River. b. An outcrop along the shore of Andrew Lake showing metasedimentary schlieren deformed along with the enveloping granite. c. Well-foliated paragneiss cross-cut by a late dike of granite. d. Mylonitic paragneiss and granite. e. Elongate grains of garnet in the foliation plane. f. Garnet-bearing leucosomes in high-grade paragneiss. g and h. Deformed leucosome with asymmetrical tails.

Figure 3 illustrates some of the contact relationships between the paragneiss and enveloping rocks. Figure 3a shows rafts of pelitic paragneiss in weakly to undeformed Slave granitic rocks. Veins of granitic material from the paragneiss can be traced into the enveloping granitic rocks. The same high-temperature (Spl + Qtz)-bearing assemblage is found in both the paragneiss and the granitic rocks at this location, consistent with derivation of the granitic rocks *via* anatexis of the paragneiss (Chacko *et al.* 1994, Chacko & Creaser 1995, Chacko 1997). Figure 3c shows an undeformed body of granitic pegmatite cutting across a high-grade foliation, indicating the local persistence of igneous activity after high-grade metamorphism. Figures 3b and 3d show granitic rocks and high-grade paragneiss deformed together, which suggests a contemporaneous relationship among metamorphism, deformation, and igneous intrusion. These field relationships, combined with results on geochronology discussed below, suggest that high-grade metamorphism and associated anatexis may have contributed to the genesis of plutons in the southern TMZ.

## Regional Metamorphism

Previous studies of the metamorphic history of the southern TMZ include those of Godfrey & Langenberg (1978), Nielsen *et al.* (1981), Langenberg & Nielsen (1982), Chacko *et al.* (1994), Chacko & Creaser (1995), and Farquhar *et al.* (1996). The high-grade mineral assemblages in metapelitic rocks throughout the southern TMZ are all indicative of granulite-facies metamorphism. The minerals in these metapelitic rocks include garnet (Grt), biotite (Bt), cordierite (Crd), sillimanite (Sil), spinel (Spl), potassium feldspar (Kfs), plagioclase (Pl), ilmenite (Ilm), quartz (Qtz) and corundum (Crn). Assemblages of metamorphic minerals were divided into four different types on the basis of their metamorphic minerals and, in particular, the textural relations of biotite and spinel. Systematic distribution of different minerals across the area (Fig. 2) suggests an overall increase in metamorphic grade, from lower granulite facies in the east to upper granulite facies in the west, although the age of metamorphism was not the same across the area (see below).

### *Mineral assemblage 1*

The westernmost, and highest grade, mineral assemblage consists of Spl + Qtz + Grt + Crd + Pl + Kfs, all anhydrous phases (Figs. 4a, b). In many samples, spinel and quartz are in apparent textural equilibrium, suggesting that they coexisted stably during peak metamorphism. This mineral assemblage implies that minimum P–T conditions of the generalized reaction:

$$\text{Grt} + \text{Crd} + \text{Sil} = \text{Spl} + \text{Qtz} \qquad (1)$$

may have been attained (Fig. 5), although the stoichiometry of this reaction is dependent on the Fe/(Fe + Mg) value of the coexisting minerals. With one exception, this mineral assemblage is limited to paragneiss associated with the western Slave granitic rocks. The regional distribution of this mineral assemblage is unusual because is represents a univariant assemblage in the FMAS system. Its widespread occurrence in the southern TMZ may be related to the presence of additional components, such as Zn or $Fe^{3+}$ in spinel (Table 5) or Ca and Mn in garnet (Table 1) acting to stabilize these phases, or possibly to arrested reaction involving those phases. The significance of this assemblage in relation to the genesis of the Slave–Province granitic rocks is discussed by Chacko (1997). Trace amounts of biotite may be present in this mineral assemblage, but it appears texturally to be of retrograde origin.

### *Mineral assemblage 2*

A mineral assemblage similar to type 1, but in which biotite is more abundant, is generally located to the east of the anhydrous type-1 mineral assemblage. In these assemblages, biotite is present as a coarsely crystalline phase parallel to the dominant foliation in the rock (Fig. 4c). Whether the biotite was stable at peak P–T conditions, or represents a high-temperature retrograde phase, is difficult to determine, but we regard its regionally greater modal abundance compared to assemblage 1 as significant.

### *Mineral assemblage 3*

In the next mineral zone to the east, spinel + quartz are no longer in apparent textural equilibrium. In these rocks, spinel is found in trace amounts as inclusions in cordierite or garnet. Spinel inclusions are typically associated with abundant inclusions of sillimanite in cordierite (Fig. 4d). In some cases, sillimanite is only found as an inclusion phase in garnet or cordierite, and is not present in the matrix.

### *Mineral assemblage 4*

The fourth metamorphic zone is characterized by the mineral assemblage Grt + Crd + Sil + Kfs + Bt + Pl + Qtz + Ilm. Spinel is not present in these rocks. The stable coexistence of these phases in apparent textural equilibrium implies that P–T conditions for the reaction:

$$\text{Bt} + \text{Sil} + \text{Qtz} = \text{Grt} + \text{Crd} + \text{Kfs} + H_2O \qquad (2)$$

were attained (Fig. 5). The breakdown of biotite + sillimanite to the stable association of cordierite + K-feldspar + garnet is considered to mark the transition from the upper amphibolite facies to the lower granulite facies in metapelitic rocks (*e.g.*, Yardley 1989).

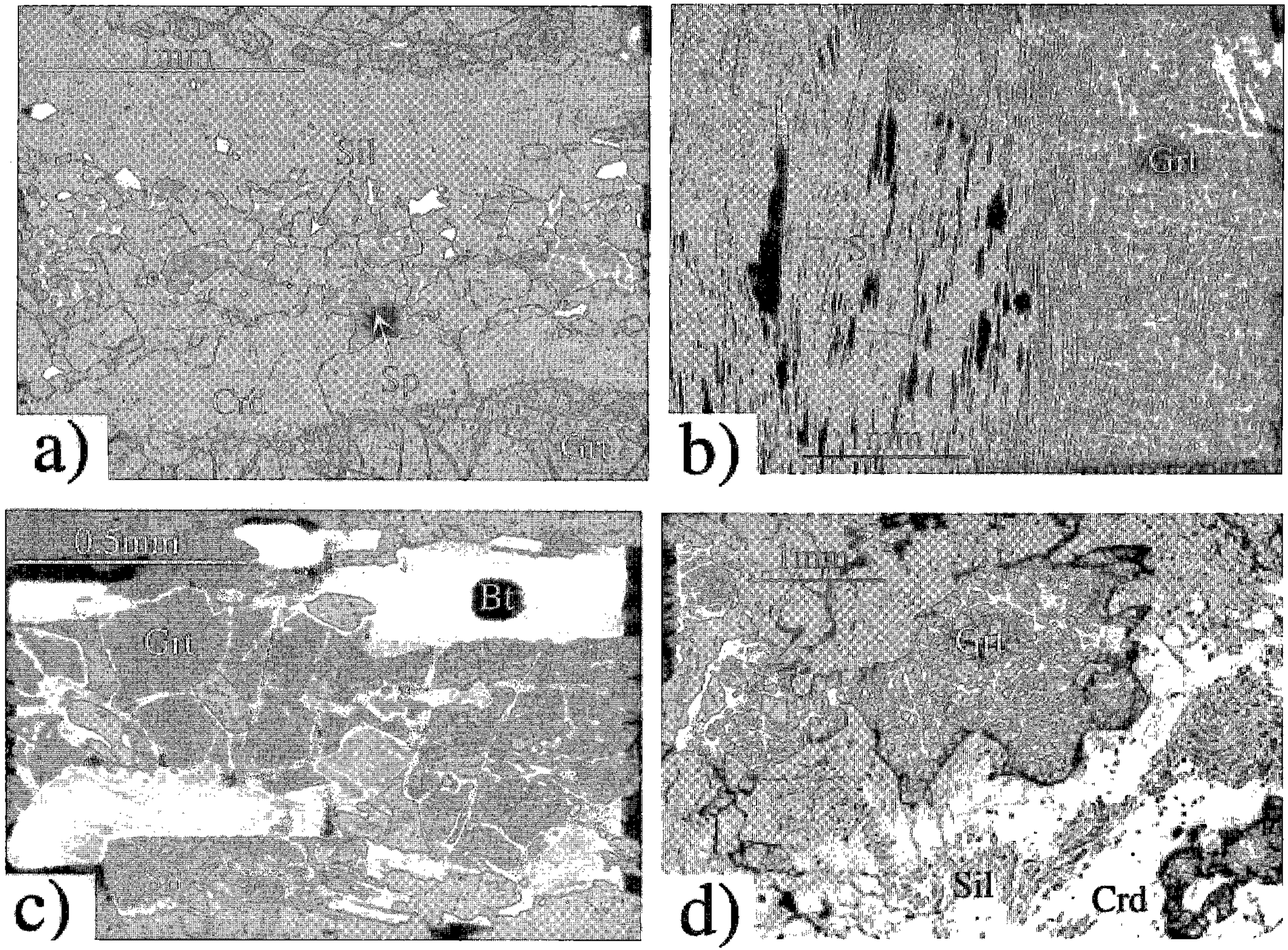


FIG. 4. Photomicrographs of granulite-facies mineral assemblages. Those shown in Figures 4a and 4b contain the assemblage Grt + Crd + Spl + Qtz + Sil + Kfs. a. Layer with the assemblage Sil + Crd + Spl sandwiched between two elongate grains of garnet. b. Strongly lineated sillimanite. c. The mineral assemblage Grt + Crd + Spl + Qtz + Sil + Kfs + Bt. Note the elongate shape of the garnet, which is characteristic of the metapelitic rocks in this area. This garnet also contains an inclusion of spinel. d. Adjacent grains of garnet and cordierite, with inclusions of sillimanite in both. Note the sillimanite-free rim around the cordierite, a common feature in many of the samples from this area.

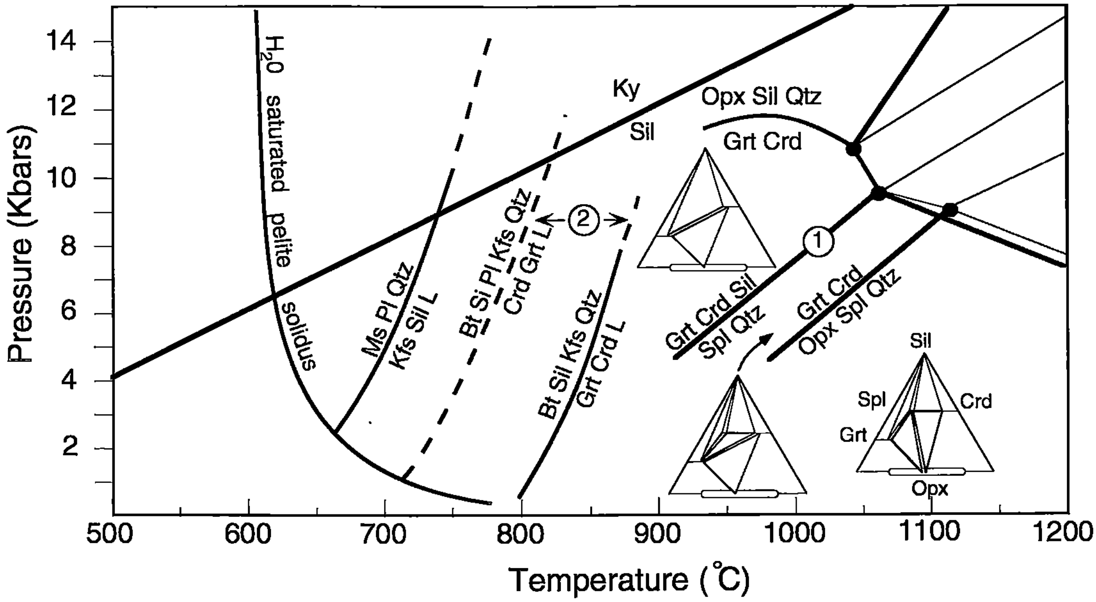


FIG. 5. Simplified phase diagram showing the experimentally determined reactions pertinent to the observed assemblages of minerals. Ms + Pl + Qtz = Kfs + Sil + L from Peto (1976). Bt + Sil + Kfs + Qtz = Crd + Grt + L (plagioclase-absent) from Carrington & Harley (1995). The position of the reaction Bt + Sil + Pl + Kfs + Qtz = Crd + Grt + L (plagioclase-bearing) is located approximately using data in Le Breton & Thompson (1988) and Vielzeuf & Holloway (1988), with slope parallel to the curve of Carrington & Harley (1995). The highest-grade Bt-absent reactions (system FMAS) are taken from Harley (1989).

The systematic variation in the assemblages of metamorphic minerals across the area represents an increase in metamorphic grade from lower to upper granulite facies from east to west across the area. For $Fe^{2+}$–Mg spinel, the stable association of the spinel + quartz assemblage requires temperatures in excess of 850°C at 5–7 kbar. Despite such extreme temperatures, orthopyroxene has not been observed in the paragneiss, most likely because of the aluminous bulk-composition.

Because the metasedimentary rocks occur in discontinuous elongate bodies parallel to the regional north-trending fabric, it is not possible to trace the change in metamorphic grade across a single unit. This makes it difficult to determine the significance of the observed regional variation in metamorphic grade. It could represent a regional variation in peak metamorphic P–T conditions, a regional variation in the activity of $H_2O$ during peak metamorphism, or systematic variation in the amount of retrogression during cooling and deformation. For example, biotite may have developed locally owing to an influx of $H_2O$ associated with the initiation of movement along shear zones. Moreover, the north-trending shear zones show evidence of a protracted period of deformation, such that the metamorphic gradient illustrated in Figure 2 may have been modified by movement along the shear zones following the peak of metamorphism, although there are no apparent breaks in assemblages across the shear zones. These alternatives are discussed below.

*Migmatization*

The presence of abundant migmatite is interpreted to reflect widespread anatexis that accompanied high-grade metamorphism. The migmatite is characterized by the development of a quartzofeldspathic leucosome spanning a continuum of scales from mm- to cm-scale patches and segregations to more continuous cm- to m-scale lenses and dikes. In the western portion of the study area, rafts of pelitic paragneiss are engulfed by the western Slave granites (Fig. 3a). The restitic rocks always have a prominent foliation regardless of whether they occur within a shear zone or away from a shear zone, suggesting that anatexis was accompanied by regional deformation. In some locations, deformed leucosomes in shear zones suggest that anatexis at least partially predated or was synchronous with movement along the shear zones. However, in other areas, the leucosomes have little to no fabric, whereas adjacent restitic rocks have a strong foliation (Figs. 3f, g). In these latter cases, either strain was heterogeneous and anatectic melts migrated to zones of low strain, or

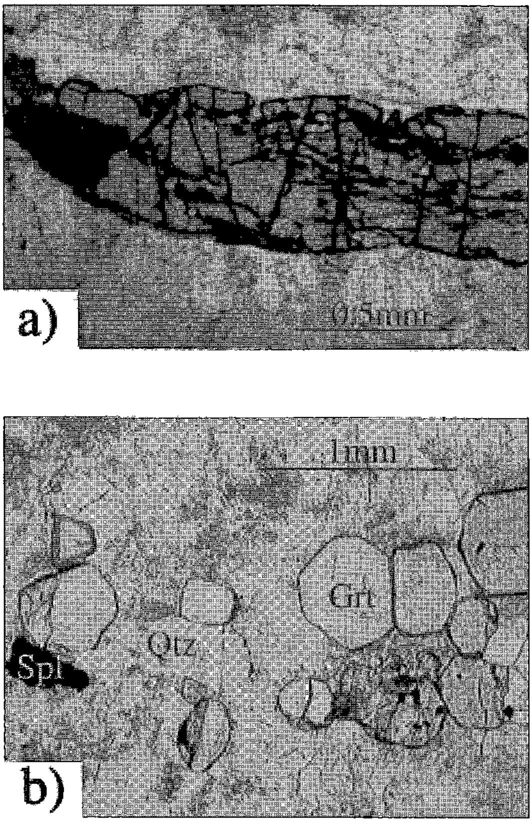


FIG. 6. Photomicrographs of garnet found in leucosomes. a. Elongate grain of garnet with inclusions of sillimanite and spinel. The texture suggests that this is relict garnet. b. Inclusion-free, euhedral grain of garnet, inferred to have been produced by the melting reaction.

the restitic rocks contain an older fabric unrelated to the shear zones.

Restites, leucosomes, and enveloping granites often contain the same phases, although in different proportions. Mineral assemblages in leucosomes are dominated by potassium feldspar, plagioclase and quartz, but they may contain lesser amounts of garnet, cordierite, sillimanite and spinel, whereas the restitic assemblages are dominated by these phases. Grains of garnet in the restite are typically elongate in the foliation plane (Figs. 3e, 6a), whereas those in the leucosome tend to be more equant (Fig. 6b). In many samples, garnet in the restite has abundant inclusions of sillimanite, whereas no inclusions are present in garnet in the leucosome (Fig. 6). The spatial association of more equant garnet with the leucosome is consistent with growth of garnet as a result of partial melting (*e.g.*, Powell & Downes 1990). Le Breton & Thompson (1988) and Patiño Douce & Johnston (1991) demonstated that garnet can grow as a result of incongruent dehydration of biotite *via* a reaction of the form:

biotite + sillimanite + orthoclase + plagioclase
+ quartz = garnet + cordierite + melt (3).

The approximate position of this reaction is illustrated in Figure 3.

Several lines of evidence suggest that the paragneisses may represent a portion of the parent material from which the granitic magmas were derived during widespread granulite-facies metamorphism and anatexis (Chacko & Creaser 1995, Chacko *et al.* 1994, Chacko 1997, De *et al.* 1997): the common association of migmatitic paragneiss with bodies of granitic rocks, the high-temperature assemblages of minerals preserved in the paragneisses, and the fact that some of the granitic rocks commonly contain many of the same mineral phases found in the paragneisses, such as garnet, cordierite, sillimanite and, more rarely, spinel. This interpretation is supported for the Slave granitic suites in the TMZ by isotopic studies, which show that the granites were generated by partial melting of a metasedimentary protolith in the lower crust (Chacko & Creaser 1995, Chacko *et al.* 1994, Thériault 1992).

## QUANTITATIVE ASSESSMENT OF METAMORPHIC EVOLUTION

The mineral assemblages in the pelitic paragneisses allow for quantitative estimation of peak pressures and temperatures of metamorphism using geothermobarometric calculations. Traditionally, metamorphic pressures and temperatures have been determined using the intersection of two equilibria, a temperature-sensitive Fe–Mg exchange geothermometer that has a relatively steep slope in P–T space and a pressure-sensitive solid–solid net-transfer reaction that has a relatively shallow slope in P–T space. More recent techniques involve the examination of all possible equilibria, or minimization of free energies of all possible species, within a given mineral assemblage (*e.g.*, Berman 1991, Gordon 1992, Holland & Powell 1991). We used the TWQ software of Berman (1991) and the thermodynamic database of Berman & Aranovich (1996).

The difficulties of applying geothermobarometric techniques to granulite-facies metamorphic rocks are well documented (Frost & Chacko 1989, Spear & Florence 1992, Pattison & Bégin 1994, Fitzsimons & Harley 1994). One of the primary difficulties reflects the different rates of diffusion for different elements, which means that during cooling from peak conditions, some elements continue to exchange (*e.g.*, Fe–Mg) after others have ceased exchanging (*e.g.*, Ca in Grt, and Al in Opx: Pattison & Bégin 1994). This situation violates the assumption of equilibrium (simultaneous equilibration of all elements in all phases, or selected

TABLE 1. COMPOSITION OF GARNET, AVERAGE OF CORE COMPOSITIONS*, SOUTHERN TALTSON MAGMATIC ZONE

| | MSB93-T54D | (N=11) | MSB93-18 | (N=35) | MSB93-T52 | (N=20) | MSB93-T2A | (N=25) | MSB93-T11A | (N=27) | VAN53B | (N=7) |
|---|---|---|---|---|---|---|---|---|---|---|---|---|
| $SiO_2$ | 38.54 | (0.30) | 38.00 | (0.31) | 37.94 | (0.28) | 38.57 | (0.25) | 38.27 | (0.31) | 38.35 | (0.20) |
| $Al_2O_3$ | 21.75 | (0.27) | 21.22 | (0.29) | 20.96 | (0.18) | 21.61 | (0.26) | 21.52 | (0.28) | 21.38 | (0.19) |
| FeO | 33.09 | (0.18) | 35.25 | (0.40) | 36.20 | (0.18) | 32.95 | (0.37) | 33.20 | (0.39) | 32.48 | (0.33) |
| MnO | 0.46 | (0.04) | 0.98 | (0.03) | 0.70 | (0.10) | 0.52 | (0.02) | 0.55 | (0.02) | 0.25 | (0.01) |
| MgO | 6.83 | (0.05) | 5.22 | (0.18) | 4.73 | (0.04) | 6.82 | (0.17) | 6.56 | (0.17) | 7.03 | (0.09) |
| CaO | 1.17 | (0.18) | 0.60 | (0.06) | 0.84 | (0.03) | 1.32 | (0.07) | 1.07 | (0.21) | 1.43 | (0.06) |
| Total | 101.84 | (0.35) | 101.31 | (0.53) | 101.38 | (0.44) | 101.79 | (0.58) | 101.18 | (0.61) | 100.92 | (0.47) |
| | MLL5 | (N=17) | TLL-8 | (N=13) | TCH51B | (N=5) | JG-654 | (N=34) | JG449 | (N=14) | JG-568 | (N=11) |
| $SiO_2$ | 37.97 | (0.33) | 37.41 | (0.41) | 36.95 | (0.36) | 38.22 | (0.32) | 38.04 | (0.16) | 37.81 | (0.25) |
| $Al_2O_3$ | 21.44 | (0.25) | 21.47 | (0.55) | 20.67 | (0.34) | 21.26 | (0.20) | 21.30 | (0.21) | 21.34 | (0.22) |
| FeO | 34.93 | (0.19) | 36.92 | (0.57) | 37.29 | (0.55) | 35.57 | (0.28) | 37.00 | (0.21) | 35.31 | (0.19) |
| MnO | 1.65 | (0.03) | 0.40 | (0.04) | 0.59 | (0.12) | 0.46 | (0.02) | 0.34 | (0.03) | 0.97 | (0.04) |
| MgO | 4.94 | (0.08) | 4.43 | (0.12) | 3.55 | (0.20) | 5.56 | (0.17) | 4.70 | (0.09) | 4.99 | (0.14) |
| CaO | 1.00 | (0.03) | 0.84 | (0.02) | 0.89 | (0.02) | 0.49 | (0.03) | 0.90 | (0.02) | 0.86 | (0.03) |
| Total | 101.97 | (0.44) | 101.48 | (1.15) | 99.94 | (0.71) | 101.57 | (0.48) | 102.28 | (0.38) | 101.29 | (0.65) |

* Standard deviation reported in parentheses. Compositions reported in wt.%.

parts, at the same temperature), and results in potentially meaningless P–T results.

Electron-microprobe traverses across garnet and cordierite crystals from the metapelitic rocks reveal that these minerals are chemically zoned. Garnet crystals commonly show an increase in the Fe/Mg ratio from core to rim, whereas cordierite crystals show the opposite trend. These features suggest that there has been significant retrograde re-equilibration of Fe and Mg upon cooling from granulite-grade metamorphic temperatures. Even crystals surrounded by non-(Fe,Mg)-bearing phases show some Fe–Mg zoning, suggesting that Fe–Mg re-equilibration occurred on at least a thin-section scale and not only between adjacent Fe–Mg mineral phases.

We assumed that the compositions least affected by re-equilibration would be those in the core of the largest crystals, especially those not in contact with other Fe–Mg minerals. However, recognizing that even the core of large grains may be affected by late Fe–Mg exchange (*e.g.*, Bégin & Pattison 1994, Pattison & Bégin 1994), our estimates of temperature must be regarded as minimum estimates.

*Analytical method and approach in modeling*

All minerals were analyzed using the ARL–SEMQ microprobe at the University of Calgary. Analyses were conducted using a 2–10 μm spot size, and counting times of 20 seconds for each element. Well-characterized natural mineral standards were used to determine mineral compositions [see Nicholls & Stout (1988) for typical operating conditions, precision and detection limits]. Mineral compositions used in the thermobarometric calculations are listed in Tables 1–5. The compositions presented for garnet and cordierite are average compositions of the cores of large crystals.

TABLE 2. COMPOSITION OF BIOTITE*, SOUTHERN TALTSON MAGMATIC ZONE

| | JG568 | (N=9) | JG-654 | (N=23) | MSB93 | (N=9) | MSB93 | (N=20) | MSB93 | (N=15) | TCH- | (N=4) | VAN53 | (N=) | JG74- | (N=6) |
|---|---|---|---|---|---|---|---|---|---|---|---|---|---|---|---|---|
| | | | | | -T2A | | -T11A | | -T52 | | 51-B | | B | | 449 | |
| $SiO_2$ | 35.64 | (0.21) | 37.88 | (0.30) | 36.83 | (0.30) | 36.21 | (0.59) | 36.03 | (0.38) | 34.22 | (0.09) | 35.67 | (0.47) | 35.16 | (0.13) |
| $TiO_2$ | 3.53 | (0.53) | 3.64 | (0.38) | 3.49 | (0.50) | 3.15 | (0.28) | 3.51 | (0.24) | 2.93 | (0.10) | 2.91 | (0.28) | 3.42 | (0.24) |
| $Al_2O_3$ | 17.96 | (0.90) | 15.63 | (0.36) | 17.44 | (0.41) | 18.26 | (0.56) | 17.67 | (0.24) | 19.57 | (0.47) | 18.46 | (0.90) | 18.73 | (0.14) |
| FeO | 18.60 | (0.93) | 15.07 | (0.39) | 17.01 | (0.14) | 16.60 | (0.48) | 19.17 | (0.28) | 20.85 | (0.01) | 17.36 | (0.50) | 21.92 | (0.49) |
| MnO | 0.05 | (0.01) | 0.02 | (0.01) | 0.03 | (0.01) | 0.02 | (0.01) | 0.02 | (0.01) | 0.02 | (0.01) | 0.01 | (0.01) | 0.01 | (0.01) |
| MgO | 9.49 | (0.50) | 14.15 | (0.56) | 12.26 | (0.38) | 11.69 | (0.28) | 10.81 | (0.29) | 8.35 | (0.07) | 10.64 | (0.39) | 7.39 | (0.39) |
| CaO | 0.03 | (0.02) | 0.01 | (0.01) | 0.02 | (0.01) | 0.02 | (0.01) | 0.01 | (0.01) | 0.02 | (0.01) | 0.01 | (0.01) | 0.02 | (0.02) |
| $Na_2O$ | 0.12 | (0.05) | 0.08 | (0.02) | 0.04 | (0.01) | 0.14 | (0.03) | 0.09 | (0.01) | 0.08 | (0.01) | 0.05 | (0.02) | 0.06 | (0.02) |
| $K_2O$ | 9.83 | (0.16) | 9.88 | (0.26) | 9.97 | (0.18) | 10.04 | (0.16) | 9.96 | (0.22) | 9.38 | (0.06) | 9.97 | (0.20) | 9.80 | (0.13) |
| F | 1.16 | (0.18) | 3.44 | (0.21) | 1.80 | (0.11) | 0.63 | (0.08) | 1.34 | (0.10) | 0.42 | (0.04) | 0.72 | (0.09) | 0.53 | (0.07) |
| $H_2O$ | 3.44 | (0.15) | 2.43 | (0.10) | 3.20 | (0.06) | 3.71 | (0.04) | 3.38 | (0.05) | 3.71 | (0.02) | 3.61 | (0.08) | 3.68 | (0.05) |
| TOTAL | 99.85 | (0.92) | 99.17 | (0.62) | 100.49 | (0.65) | 99.91 | (0.78) | 100.81 | (0.787) | 99.16 | (0.37) | 98.76 | (1.01) | 100.24 | (0.92) |

* Standard deviation reported in parentheses. Compositions quoted in wt.%.

TABLE 3. COMPOSITION OF PLAGIOCLASE*, SOUTHERN TALTSON MAGMATIC ZONE

| | TCH-51-B2 | (N=11) | VAN53 B | (N=4) | MSB93 -T54D | (N=11) | MSB93 -T2A | (N=21) | MSB93 -T52 | (N=9) | JG-654 | (N=24) | MSB93 -T11A | (N=4) | JG449 | (N=5) | JG-568 | (N=30) |
|---|---|---|---|---|---|---|---|---|---|---|---|---|---|---|---|---|---|---|
| $SiO_2$ | 60.82 | (0.66) | 60.90 | (0.27) | 58.72 | (0.23) | 56.95 | (0.36) | 61.41 | (0.28) | 63.48 | (0.58) | 62.80 | (0.28) | 63.63 | (1.35) | 61.36 | (0.37) |
| $Al_2O_3$ | 24.11 | (0.50) | 24.95 | (0.29) | 27.05 | (0.21) | 27.42 | (0.21) | 24.64 | (0.25) | 22.79 | (0.47) | 23.23 | (0.07) | 23.67 | (1.17) | 24.32 | (0.28) |
| FeO | 0.13 | (0.16) | 0.31 | (0.13) | 0.10 | (0.04) | 0.03 | (0.02) | 0.01 | (0.01) | 0.02 | (0.03) | 0.05 | (0.02) | 0.06 | (0.04) | 0.03 | (0.03) |
| CaO | 5.99 | (0.07) | 6.13 | (0.12) | 8.46 | (0.22) | 8.71 | (0.17) | 5.85 | (0.05) | 4.12 | (0.45) | 4.45 | (0.11) | 4.51 | ((1.13) | 5.76 | (0.18) |
| $Na_2O$ | 8.19 | (0.09) | 8.40 | (0.05) | 6.91 | (0.09) | 6.52 | (0.06) | 8.29 | (0.10) | 9.34 | (0.27) | 9.04 | (0.12) | 9.20 | (0.65) | 8.34 | (0.18) |
| $K_2O$ | 0.06 | (0.03) | 0.14 | (0.02) | 0.15 | (0.13) | 0.15 | (0.04) | 0.19 | (0.03) | 0.23 | (0.17) | 0.23 | (0.01) | 0.12 | (0.03) | 0.26 | (0.21) |
| TOTAL | 99.33 | (1.14) | 100.83 | (0.60) | 101.39 | (0.35) | 99.79 | (0.53) | 100.40 | (0.34) | 99.99 | (0.57) | 99.78 | (0.23) | 101.19 | (0.52) | 100.07 | (0.55) |

* Standard deviation reported in parentheses. Compositions quoted in wt.%.

TABLE 4. COMPOSITION OF CORDIERITE*,
SOUTHERN TALTSON MAGMATIC ZONE

| | TCH-51-B | (N=9) | MSB93 -T54D | (N=10) | MSB93 -18 | (N=16) | MSB93 -T52 | (N=8) | MSB93 -T2A | (N=12) | MSB93 -T11A | (N=12) |
|---|---|---|---|---|---|---|---|---|---|---|---|---|
| $SiO_2$ | 47.47 | (0.54) | 48.00 | (0.33) | 47.74 | (0.52) | 47.49 | (0.21) | 48.52 | (0.27) | 47.58 | (0.33) |
| $Al_2O_3$ | 34.43 | (0.46) | 33.32 | (0.28) | 32.66 | (0.47) | 32.68 | (0.39) | 33.45 | (0.31) | 32.56 | (0.35) |
| FeO | 10.16 | (0.13) | 8.45 | (0.12) | 9.77 | (0.10) | 9.96 | (0.08) | 8.92 | (0.07) | 7.99 | (0.11) |
| MnO | 0.03 | (0.01) | 0.04 | (0.01) | 0.09 | (0.01) | 0.06 | (0.01) | 0.05 | (0.01) | 0.04 | (0.01) |
| MgO | 7.11 | (0.10) | 8.55 | (0.10) | 7.74 | (0.18) | 7.49 | (0.08) | 8.53 | (0.09) | 8.72 | (0.15) |
| CaO | 0.01 | (0.00) | 0.01 | (0.01) | 0.01 | (0.02) | 0.00 | (0.00) | 0.00 | (0.00) | 0.01 | (0.01) |
| $Na_2O$ | 0.17 | (0.02) | 0.08 | (0.01) | 0.04 | (0.02) | 0.10 | (0.01) | 0.05 | (0.02) | 0.18 | (0.11) |
| $K_2O$ | 0.00 | (0.00) | 0.00 | (0.00) | 0.00 | (0.00) | 0.00 | (0.00) | 0.00 | (0.00) | 0.00 | (0.00) |
| TOTAL | 99.38 | (0.81) | 98.44 | (0.58) | 98.05 | (0.97) | 97.78 | (0.41) | 99.53 | (0.40) | 97.08 | (0.46) |

| | JG449 | (N=8) | JG568 | (N=17) | VAN53 B | (N=6) | MLL5 | (N=10) | TLL-8-1 | (N=8) |
|---|---|---|---|---|---|---|---|---|---|---|
| $SiO_2$ | 47.47 | (0.37) | 47.16 | (0.39) | 46.45 | (0.28) | 47.44 | (0.40) | 47.38 | (0.42) |
| $Al_2O_3$ | 32.72 | (0.37) | 32.76 | (0.23) | 33.37 | (0.36) | 32.77 | (0.33) | 35.49 | (0.58) |
| FeO | 11.17 | (0.11) | 9.83 | (0.22) | 8.08 | (0.20) | 10.88 | (0.15) | 11.40 | (0.25) |
| MnO | 0.06 | (0.01) | 0.11 | (0.01) | 0.02 | (0.01) | 0.16 | (0.02) | 0.03 | (0.01) |
| MgO | 6.96 | (0.04) | 7.25 | (0.20) | 8.12 | (0.15) | 7.12 | (0.11) | 6.50 | (0.14) |
| CaO | 0.00 | (0.00) | 0.01 | (0.01) | 0.00 | (0.00) | 0.00 | (0.00) | 0.01 | (0.00) |
| $Na_2O$ | 0.06 | (0.01) | 0.21 | (0.13) | 0.03 | (0.01) | 0.04 | (0.02) | 0.05 | (0.01) |
| $K_2O$ | 0.00 | (0.00) | 0.00 | (0.00) | 0.01 | (0.01) | 0.00 | (0.00) | 0.01 | (0.01) |
| TOTAL | 98.44 | (0.59) | 97.33 | (0.65) | 96.08 | (0.42) | 98.42 | (0.68) | 100.87 | (1.12) |

* Standard deviation reported in parentheses. Compositions reported in wt.%.

TABLE 5. COMPOSITION OF SPINEL*, SOUTHERN TALTSON MAGMATIC ZONE

| | MLL5 | (N=17) | MSB93-18 | (N=35) | MSB93-T52 | (N=20) | MSB93-T2A | (N=25) | JG-654 | (N=4) | MSB93-T11A | (N=27) | JG-568 | (N=11) |
|---|---|---|---|---|---|---|---|---|---|---|---|---|---|---|
| $SiO_2$ | 0.00 | (0.00) | 38.00 | (0.31) | 37.94 | (0.28) | 38.57 | (0.25) | 0.00 | (0.00) | 38.27 | (0.31) | 37.81 | (0.25) |
| $Al_2O_3$ | 55.01 | (0.62) | 21.22 | (0.29) | 20.96 | (0.18) | 21.61 | (0.26) | 57.47 | (0.36) | 21.52 | (0.28) | 21.34 | (0.22) |
| FeO | 40.60 | (0.62) | 35.25 | (0.40) | 36.20 | (0.18) | 32.95 | (0.37) | 32.79 | (0.53) | 33.20 | (0.39) | 35.31 | (0.19) |
| MnO | 0.14 | (0.03) | 0.98 | (0.03) | 0.70 | (0.10) | 0.52 | (0.02) | 0.04 | (0.01) | 0.55 | (0.02) | 0.97 | (0.04) |
| MgO | 3.25 | (0.45) | 5.22 | (0.18) | 4.73 | (0.04) | 6.82 | (0.17) | 3.45 | (0.41) | 6.56 | (0.17) | 4.99 | (0.14) |
| ZnO | 0.34 | (0.07) | 0.60 | (0.06) | 0.84 | (0.03) | 1.32 | (0.07) | 5.39 | (0.55) | 1.07 | (0.21) | 0.86 | (0.03) |
| Total | 99.34 | (0.43) | 101.31 | (0.53) | 101.38 | (0.44) | 101.79 | (0.58) | 99.15 | (0.42) | 101.18 | (0.61) | 101.29 | (0.65) |

* Standard deviation reported in parentheses. Compositions quoted in wt.%.

TABLE 6. CALCULATED P–T RESULTS, SOUTHERN TALTSON MAGMATIC ZONE

| Sample | Temperature (°C) | Pressure (kbar) |
|---|---|---|
| MSB93-T54D | 880 | 7.1 |
| MSB93-T2A* | 880 | 7.2 |
| TLL-8 | 870 | 6.6 |
| MLL-5 | 870 | 6.5 |
| MSB93-T52* | 830 | 6.3 |
| VAN53B* | 780 | 6.9 |
| TCH51B* | 810 | 6.0 |
| MSB93-T11A* | 730 | 6.5 |
| JG449* | 810 | 6.2 |
| JG568* | 770 | 5.8 |
| MSB93-18 | 820 | 6.3 |
| JG568* | 840 | 6.4 |
| JG654** | 610 | 2.9 |

Temperatures rounded to nearest ten degrees. All samples contain Grt+Sil+Pl+Qtz+Crd.
* Samples contain Bt not used in the P-T calculations.
** Sample contains no Crd; Bt was used in P-T calculations

P–T calculations were performed with the TWQ software program (Berman 1991) using internally consistent thermodynamic data for end members and solid solutions (TWQ version 2.02). These data account for nonideal mixing of Fe–Mg in cordierite and Fe–Mg–Ca in garnet (Berman & Aranovich 1996), as well as Fe–Mg–Ti–Al in biotite (Berman & Aranovich, unpubl. data). Spinel was not included in the P–T calculations because of the added uncertainty stemming from the effects of minor components. The P–T results are listed in Table 6 and were attained using the INTERSX program of Berman (1991).

### *Results of the modeling*

Figure 7a is a typical example illustrating the positions of calculated equilibria for individual samples from this study. This sample contains the highest-grade mineral assemblage in the area, Spl + Qtz + Grt + Crd + Sil + Pl + Kfs. Figure 7b is a similar diagram for a biotite-bearing sample. Overall, the agreement between the two barometers shown in Figures 7a and 7b is excellent. Grt–Bt temperatures, however, are generally lower than Grt–Crd temperatures. This discrepancy is most likely due to the significant F content of the biotite in the TMZ assemblages, a compositional effect that can increase temperatures by as much as 40–50°C per 0.1 mole fraction F (Aranovich 1991). This interpretation is consistent with the fact that the lowest temperature is calculated for sample JG654, the one with the highest F content. However, the lower garnet – biotite temperatures may also be due to down-temperature Fe–Mg exchange between garnet and biotite or post-peak metamorphic growth of biotite during high-temperature deformation along the shear zone.

The regional distribution of the results of our calculations is shown in Figure 2. The spinel-bearing mineral assemblages consistently yield the highest metamorphic temperatures, generally above 850°C at pressures of 5–7 kbars. As minimum estimates, these results are consistent with minimum estimates of temperature of 850–900°C at 5–7 kbar for Spl + Qtz assemblages from experimentally constrained petrogenetic grids in FMAS space (Fig. 5), recognizing that multivariancy makes reaction 1 less well constrained than implied in Figure 5. Temperature estimates from samples containing the mineral assemblage Grt + Bt + Crd + Sil without spinel are consistently lower, averaging approximately 750°C; as minimum estimates of temperature, these results are consistent with minimum temperatures of 750–800°C for this assemblage from petrogenetic grids (reaction 2 in Fig. 5).

## METAMORPHIC EVOLUTION OF SHEAR ZONES

Assemblages of metamorphic minerals from metapelitic rocks found within the north-trending shear zones suggest a range in grade from granulite to greenschist facies. This suggests that deformation in the shear zones began while the rocks were at or near peak temperatures of metamorphism, and persisted as they cooled.

The occurrence of deformation at granulite grade within the shear zones is supported by field and petrographic observations. Granulite-facies mineral assemblages exhibit a strong penetrative fabric, and locally, within the Leland Lakes and Charles Lake shear zones, exhibit mylonitic fabrics. Figure 4a, a photomicrograph of garnet, spinel, cordierite, and sillimanite, displays a prominent foliation, which is suggestive of recrystallization during deformation. Subhorizontal, strike-lineated coarse-grained crystals of sillimanite are found along several of the shear zones (Fig. 4b). Grains of garnet 3–4 cm in length are elongate in the plane of the foliation (Fig. 3e). These elongate grains of garnet also contain aligned inclusions of sillimanite, suggesting that mineral growth was accompanied by deformation. The high-grade paragneiss also is commonly associated with sheared granitic rocks containing megacrystic K-feldspar crystals that experienced ductile deformation (McDonough *et al.* 1997), indicating deformation under high-temperature conditions.

Successive overprinting of progressively lower-grade assemblages of metamorphic minerals on the original granulite-facies assemblages indicates continued shear-zone movement as the rocks cooled. Figure 8a is a photomicrograph of a brittly deformed, fractured porphyroblast of garnet contained in the peak assemblage Grt + Bt + Kfs + Crd + Sil + Qtz + Pl. Within the fractures, garnet is replaced by biotite + sillimanite. The high-temperature replacement of garnet by biotite

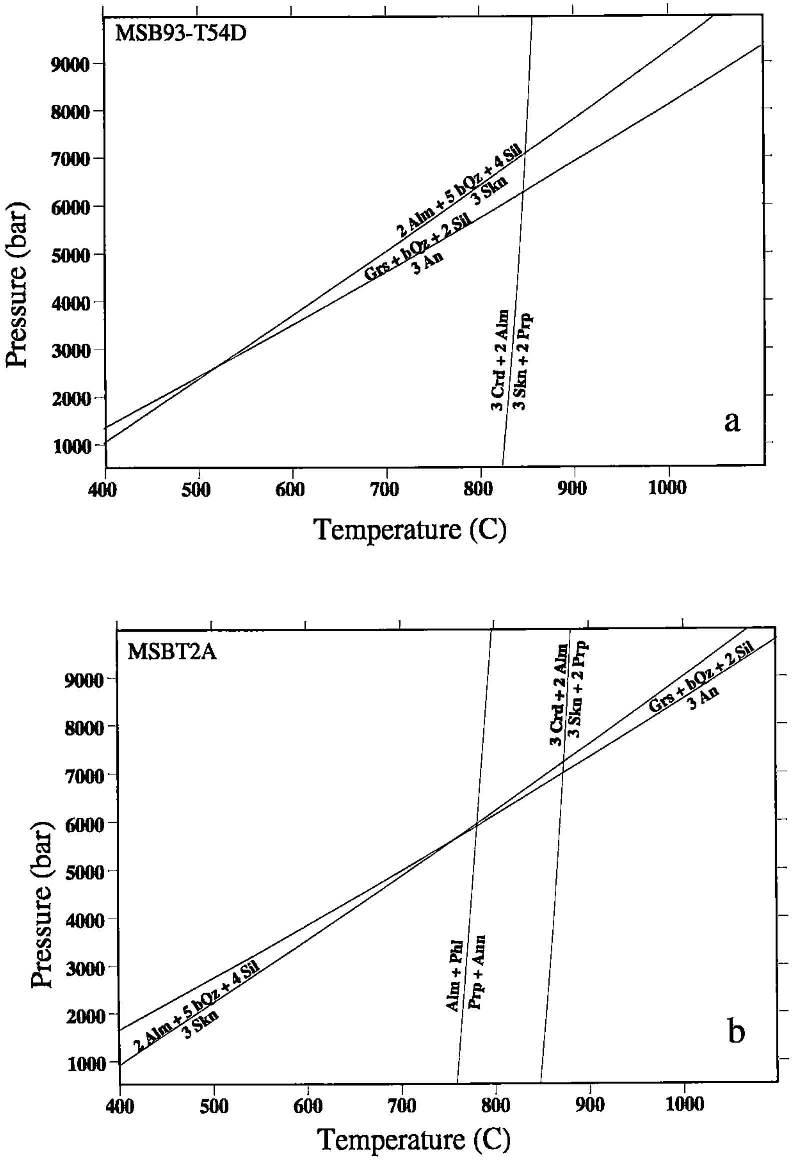


FIG. 7. a. Phase diagram illustrating the position of the calculated equilibria for sample MSB93-T54D, which contains the assemblage Grt + Sil + Spl + Crd + Pl + Qtz. The number of independent equilibria for this assemblage equals 3. b. Phase diagram illustrating the positions of the calculated equilibria for sample MSBT2A, which contains the above assemblage plus biotite. There are four independent equilibria for this assemblage. Skn stands for sekaninaite, the Fe end-member of cordierite.

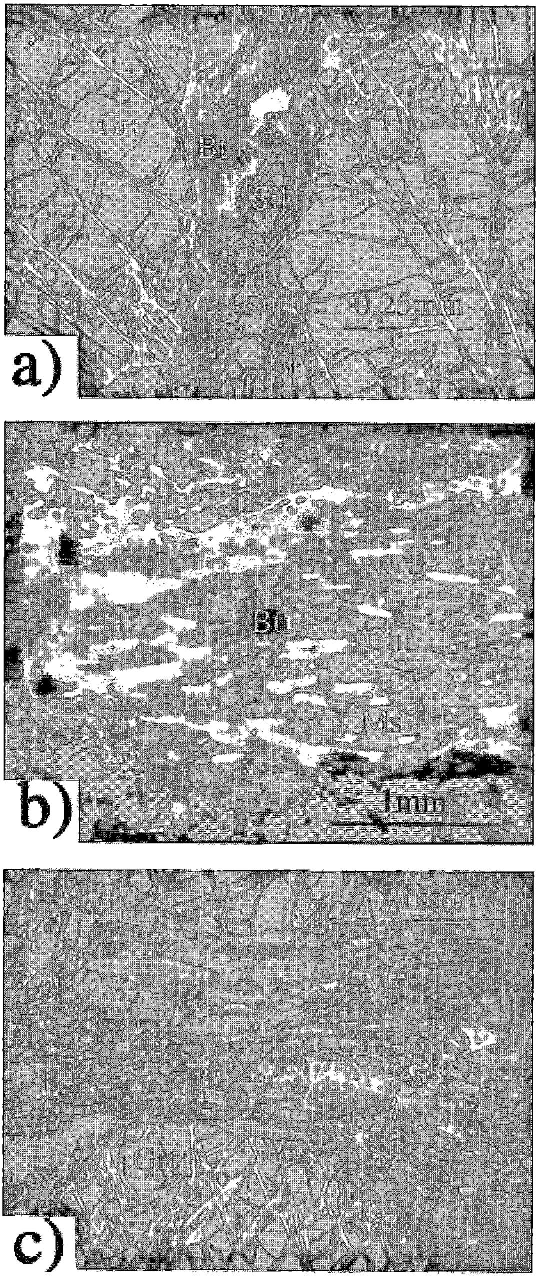


FIG. 8. Photomicrographs illustrating the overprinting of granulite-facies mylonites by lower-grade assemblages. a. Secondary biotite and sillimanite growing in the fracture of a deformed grain of garnet. b. The replacement of cordierite by biotite and chlorite. c. Fine-grained muscovite replacing K-feldspar.

and sillimanite may have taken place during retrograde metamorphism *via* the reverse of reaction 2, that defines the transition from the granulite to the amphibolite facies.

Other samples within the shear zones show evidence of retrogression at still lower temperatures. Many sillimanite-bearing samples contain coarse-grained muscovite, which replaces K-feldspar (Plint & McDonough 1995, Fig. 2b). The coarse-grained nature of the muscovite suggests that it grew during relatively high-temperature rehydration and breakdown of K-feldspar, perhaps *via* the reaction:

$$\mathrm{Kfs + Sil + H_2O = Ms + Qtz} \qquad (4)$$

Granulite- and amphibolite-facies mylonites are variably, commonly pervasively, overprinted by greenschist-facies mylonites. Cataclastic textures associated with greenschist-facies mylonites are well developed in the megacrystic granitic rocks, where the crystals of K-feldspar are brittly fractured and sheared apart. In the metapelitic rocks, garnet and cordierite are replaced by fine-grained chlorite and biotite (Fig. 8b), and K-feldspar is replaced by fine-grained muscovite (Fig. 8c).

## TIMING OF GRANULITE-FACIES METAMORPHISM AND SHEAR-ZONE MOVEMENT

U–Pb geochronology on zircon and monazite from pelitic paragneisses and numerous intrusive rocks, combined with their respective field-relationships, constrain the timing of high-grade metamorphism and shear-zone movement. Isotopic analysis of single crystals of monazite from a sample of granulite-grade pelitic gneiss collected at Myers Lake along the Leland Lakes shear zone yields U–Pb ages between 1926 and 1923 Ma (McDonough *et al.* 1997). Monazite from a sample of high-grade pelitic gneiss from the Charles Lake shear zone yield ages between 1925 and 1919 Ma (McDonough *et al.* 1997, Fig. 12). Crystals of metamorphic monazite from samples of the TBC range in age from 1933 to 1913 Ma, suggesting that granulite-facies metamorphism occurred at approximately this time. These results contrast with the earlier estimates of approximately 2.4 Ga for the timing of granulite-facies metamorphism in this region (Godfrey & Langenberg 1978, Nielsen *et al.* 1981, Langenberg & Nielsen 1982).

The above range in ages for the timing of granulite-facies metamorphism is consistent with constraints deduced from the geochronology and field relationships of intrusive rocks. The Arch Lake pluton, which is bound on the west and the east by the Leland Lakes and Charles Lake shear zones, respectively (Fig. 2), has a mylonitic foliation in the shear zones. This foliation is comprised, in part, of ductilely deformed K-feldspar megacrysts, implying high-temperature shearing. U–Pb geochronology from zircon in the Arch Lake pluton yields an age of approximately 1938 Ma. This age is taken to represent the maximum age for granulite-grade, ductile deformation in both the Leland Lakes and Charles Lake shear zones (McDonough *et al.* 1997).

The Charles Lake granite is deformed in the Charles Lake shear zone. Unlike the Arch Lake granite, the Charles Lake granite contains amphibolite- to greenschist-grade mylonitic fabrics and shows no evidence of granulite-grade deformation. McDonough *et al.* (1997) reported an age of 1933 Ma for this granite. Dikes considered to be genetically related to the Slave pluton (McDonough *et al.* 1997) cut the high-grade fabrics associated with the Leland Lakes shear zones and are weakly to moderately foliated. One such dike yields a U–Pb age of 1934 Ma (McDonough *et al.* 1997). The above constraints suggest a lower limit on the timing of granulite-facies deformation of approximately 1933 Ma. If portions of the S-type Slave pluton were generated through anatectic melting of pelitic paragneiss, as suggested by field relationships, petrology, and isotopic data (Chacko & Creaser 1995, Chacko *et al.* 1994, Thériault 1992), this age also offers a lower constraint on the timing of regional high-grade metamorphism.

$^{40}Ar/^{39}Ar$ and K–Ar age data offer some constraints on the post-granulite-facies thermal history and amphibolite – greenschist-grade shear-zone activity. Regional hornblende-cooling ages of approximately 1900 Ma (Plint & McDonough 1995) and 1852 (Baadsgaard & Godfrey 1967) suggest a regional cooling below approximately 525°C within this time interval. Plint & McDonough (1995) interpreted the similarity of $^{40}Ar/^{39}Ar$ from hornblende on either side of the Andrew Lake shear zone as indicating a thermal spike related to the intrusion of late-tectonic anatectic granite following high-grade juxtaposition.

Secondary muscovite, formed during an amphibolite-facies overprint of a granulite-facies rock and later deformed during greenschist-grade shear-zone movement, was dated by the $^{40}Ar/^{39}Ar$ method and yields an age of 1803 Ma (Plint & McDonough 1995). Magmatic biotite from the Charles Lake granite yield $^{40}Ar/^{39}Ar$ ages of approximately 1860 and 1800 Ma (Plint & McDonough 1995). These ages are similar to the K–Ar dates, 1792 ± 40 Ma and 1772 ± 40 Ma, for muscovite and biotite, respectively, reported by Baadsgaard & Godfrey (1967). These data record a regional cooling through the 300°C isotherm at approximately 1800 Ma, suggesting that greenschist-grade mylonitization along shear zones had ceased by this time.

## Conclusions

The petrology of metapelitic enclaves present throughout the southern TMZ in northeastern Alberta, in conjunction with field observations and geochronological studies, provides constraints on the tectonothermal evolution of the crust during the development of the orogen. The pelitic paragneiss contains mineral assemblages representative of lower-granulite-facies P–T conditions in the east (Grt + Bt + Sil + Crd + Kfs + Pl) to upper-granulite-facies conditions in the west (Grt + Sil + Crd + Spl + Kfs + Pl). Geothermobarometric calculations, along with phase-diagram considerations, show that peak metamorphic temperatures were at least 750°C in the east and at least 850°C in the west at pressures of 5–7 kbars. Anatexis accompanied peak metamorphism.

Field relationships, mineral assemblages and textures, and geochronological data, are consistent with a single phase of granulite-facies metamorphism at approximately 1.93 Ga. Strike-lineated, granulite-grade mylonitic paragneiss and granitic rocks exhibiting fabrics typical of ductile deformation demonstrate that granulite-facies metamorphism was at least partially synchronous with movement along the Leland Lakes and Charles Lake shear zones.

Textures such as the growth of biotite and sillimanite in the fractures of deformed crystals of garnet, and the growth of secondary, but coarse-grained muscovite, after K-feldspar, indicates that granulite-facies mineral assemblages were overprinted by amphibolite-facies assemblages. These fabrics are found in the north-trending shear zones, indicating that movement along the shear zones continued as the crust was beginning to cool. Regional hornblende-cooling ages of *ca.* 1900 Ma (Plint & McDonough 1995) show that movement along the shear zones at amphibolite-facies conditions must have occurred prior to that time.

Granulite- and amphibolite-facies minerals are overprinted by cataclastic greenschist-facies mylonites. Greenschist-grade mylonites are characterized by abundant fine-grained muscovite, biotite and chlorite. Regional mica-cooling ages of approximately 1800 Ma (Plint & McDonough 1995) indicate cooling to greenschist-facies conditions at that time.

## Acknowledgements

We thank Gerry Ross, Tom Chacko, and Reg Thériault for their expertise in the field and for numerous discussions of the geology of the TMZ. We thank R. Berman, L. Aranovich and T. Chacko for timely and constructive reviews. Their comments and suggestions greatly improved the manuscript. This work was supported by a Lithoprobe Supporting Geoscience Grant and NSERC Research Grant 0037233 to DP.

## References

Aranovich, L.Y. (1991): *Mineral Equilibria of Multicomponent Solid Solutions.* Nauka Press, Moscow, Russia.

BAADSGAARD, H. & GODFREY, J.D. (1967): Geochronology of the Canadian Shield in northeastern Alberta. I. Andrew Lake area. *Can. J. Earth Sci.* **4**, 541-563.

BÉGIN, N.J. & PATTISON, D.R.M. (1994): Metamorphic evolution of granulites in the Minto Block, northern Quebec; extraction of peak P–T conditions taking account of late Fe–Mg exchange. *J. Metamorphic Geol.* **12**, 411-428.

BERMAN, R.G. (1991): Thermobarometry using multi-equilibrium calculations: a new technique, with petrological implications. *Can. Mineral.* **29**, 833-856.

________ & ARANOVICH, L.Y. (1996): Optimized standard state and mixing properties of minerals. I. Model calibration for olivine, orthopyroxene, cordierite, garnet, and ilmenite in the system FeO–MgO–CaO–$Al_2O_3$–$SiO_2$–$TiO_2$. *Contrib. Mineral. Petrol.* **126**, 1-24.

BOSTOCK, H.H. & VAN BREEMEN, O. (1994): Ages of detrital and metamorphic zircons and monazites from pre-Taltson magmatic zone basin at the western margin of Rae Province. *Can. J. Earth Sci.* **31**, 1353-1364.

CARRINGTON, D.P. & HARLEY, S.L. (1995): The stability of osumilite in metapelitic granulites. *J. Metamorphic Geol.* **13**, 613-625.

CHACKO, T. (1997): Ultra-high temperature metamorphism at Pelican Rapids, Taltson magmatic zone, NE Alberta: Possible implications for Early Proterozoic collisional orogens. *Geol. Assoc. Can. – Mineral. Assoc. Can., Program Abstr.* **22**, A24.

________ & CREASER, R.A. (1995): Hercynite-bearing granites and associated metasedimentary enclaves from the Taltson Magmatic Zone, Alberta, Canada: a natural example of high temperature pelite melting. *In* The Origin of Granites and Related Rocks: III Hutton Symp. (M. Brown & P.M. Piccoli, eds.). *U.S. Geol. Surv., Circ.* **1129**, 32-33 (abstr.).

________, ________ & POON, D. (1994): Spinel + quartz granites and associated metasedimentary enclaves from the Taltson magmatic zone, Alberta, Canada: a view into the root zone of a high-temperature, S-type granitic batholith. *Mineral. Mag.* **58A**, 161-162 (abstr.).

DE, SUMAN, CREASER, R., CHACKO, T. & MUEHLENBACHS, K. (1997): Nd, Pb, and O isotopic study of Taltson Magmatic Zone granites, NE Alberta: implications for the tectonic setting of the TMZ. *Geol. Assoc. Can. – Mineral. Assoc. Can., Program Abstr.* **22**, A36.

FARQUHAR, J., CHACKO, T. & ELLIS, D.J. (1996): Preservation of oxygen isotopic compositions in granulites from northwestern Canada and Enderby Land, Antarctica: implications for high-temperature isotopic thermometry. *Contrib. Mineral. Petrol.* **125**, 213-224.

FITZSIMONS, I.W.C. & HARLEY, S.L. (1994): The influence of retrograde cation exchange on granulite P–T estimates and a convergence technique for the recovery of peak metamorphic conditions. *J. Petrol.* **35**, 543-576.

FROST, B.R. & CHACKO, T. (1989): The granulite uncertainty principle: limitations on thermobarometry in granulites. *J. Geol.* **97**, 435-450.

GODFREY, J.D. (1986): Geology of the Precambrian Shield in northeastern Alberta. *Alberta Research Council.*

________ & LANGENBERG, C.W. (1978): Metamorphism in the Canadian Shield of northeastern Alberta. *Geol. Surv. Can., Pap.* **78-10**, 129-138.

GORDON, T.M. (1992): Generalized thermobarometry; solution of the inverse chemical equilibrium problem using data for individual species. *Geochim. Cosmochim. Acta* **56**, 1793-1800.

HANMER, S., BOWRING, S., VAN BREEMEN, O. & PARRISH, R. (1992b): Great Slave Lake shear zone, NW Canada: mylonitic record of Early Proterozoic continental convergence, collision and indentation. *J. Struct. Geol.* **14**, 757-773.

________, DARRACH, M. & KOPF, C. (1992a): The East Athabasca mylonite zone: an Archean segment of the Snowbird tectonic zone in northern Saskatchewan. *Geol. Surv. Can., Pap.* **92-1C**, 19-29.

HARLEY, S.L. (1989): The origin of granulites: a metamorphic perspective. *Geol. Mag.* **126**, 215-247.

HOFFMAN, P.F. (1988): United Plates of America, the birth of a craton: Early Proterozoic assembly and growth of Laurentia. *Annu. Rev. Earth Planet. Sci.* **16**, 543-603.

HOLLAND, T. & POWELL, R. (1991): An enlarged and updated internally consistent thermodynamic dataset with uncertainties and correlations: the system $K_2O$–$Na_2O$–CaO–MgO–FeO–$Fe_2O_3$–$Al_2O_3$–$TiO_2$–$SiO_2$–C–H–O. *J. Metamorphic Geol.* **8**, 89-124.

LANGENBERG, C.W. & NIELSEN, P.A. (1982): Polyphase metamorphism in the Canadian Shield of northeastern Alberta. *Alberta Research Council, Bull.* **42**, 1-80.

LE BRETON, N.L. & THOMPSON, A.B. (1988): Fluid-absent (dehydration) melting of biotite in metapelites in the early stages of crustal anatexis. *Contrib. Mineral. Petrol.* **99**, 226-237.

MCDONOUGH, M.R., MCNICOLL, V.J., SCHETSELAAR, E.M. & GROVER, T.W. (1997): Geochronological and kinematic constraints on crustal shortening and escape in a two-sided oblique-slip collisional and magmatic orogen, Paleoproterozoic Taltson magmatic zone, northeastern Alberta. *Tectonics* (in press).

NICHOLLS, J. & STOUT, M.Z. (1988): Picritic melts in Kilauea; evidence from the 1967–1968 Halemaumau and Hiiaka eruptions. *J. Petrol.* **29**, 1031-1057.

NIELSEN, P.A., LANGENBERG, C.W., BAADSGAARD, H. & GODFREY, J.D. (1981): Precambrian metamorphic conditions and crustal evolution, northeastern Alberta, Canada. *Precambrian Res.* **16**, 171-193.

PATIÑO DOUCE, A.E. & JOHNSTON, A.D. (1991): Phase equilibria and melt productivity in the pelitic system; implications for the origin of peraluminous granitoids and aluminous granites. *Contrib. Mineral. Petrol.* **107**, 202-218.

PATTISON, D.R.M. & BÉGIN, N.J. (1994): Zoning patterns in orthopyroxene and garnet in granulites: implications for geothermometry. *J. Metamorphic Geol.* **12**, 387-410.

PETO, P. (1976): An experimental investigation of melting relations involving muscovite and paragonite in the silica-saturated portion of the system $K_2O–Na_2O–Al_2O_3–SiO_2–H_2O$ to 15 kb total pressure. *In* Progress in Experimental Petrology. *U.K. Natural Environment Research Council, Progress Report of Research supported by N.E.R.C.* **4**, 41-45.

PLINT, H.E. & MCDONOUGH, M.R. (1995): $^{40}Ar/^{39}Ar$ and K–Ar age constraints on shear zone evolution, southern Taltson magmatic zone, northeastern Alberta. *Can. J. Earth Sci.* **32**, 281-291.

POWELL, R. & DOWNES, J. (1990): Garnet porphyroblast-bearing leucosomes in metapelites: mechanism, phase diagrams, and an example from Broken Hill, Australia. *In* High Temperature Metamorphism and Crustal Anatexis (J. Ashworth & M. Brown, eds.). *Mineralogical Society of Great Britain, Monogr.* **2**, 105-123.

ROSS, G.M., MILKEREIT, E., EATON, D., WHITE, D., KANASEWICH, E.R. & BURIANYK, M.J.A. (1995): Paleoproterozoic collisional orogen beneath the Western Canada sedimentary basin imaged by Lithoprobe crustal seismic-reflection data. *Geology* **23**, 195-199.

________, PARRISH, R.R., VILLENEUVE, M.E. & BOWRING, S.A. (1991): Geophysics and geochronology of the crystalline basement of the Alberta Basin, western Canada. *Can. J. Earth Sci.* **28**, 512-522.

SPEAR, F.S. & FLORENCE, F.P. (1992): Thermobarometry in granulites: pitfalls and new approaches. *Precambrian Res.* **55**, 209-241.

THÉRIAULT, R.J. (1992): Nd isotopic evolution of the Taltson Magmatic Zone, Northwest Territories, Canada: insights into Early Proterozoic accretion along the western margin of the Churchill Province. *J. Geol.* **100**, 465-475.

________ & ROSS, G.M. (1991): Nd isotopic evidence for crustal recycling in the ca. 2.0 Ga subsurface of western Canada. *Can. J. Earth Sci.* **28**, 1140-1147.

VAN BREEMEN, O., BOSTOCK, H.H. & LOVERIDGE, W.D. (1992): Geochronology of granites along the margin of the northern Taltson Magmatic Zone and western Rae Province, Northwest Territories. *In* Radiogenic Age and Isotopic Studies: Report 5. *Geol. Surv. Can., Pap.* **91-2**, 17-24.

VIELZEUF, D. & HOLLOWAY, J.R. (1988): Experimental determination of the fluid-absent melting relations in the pelitic system. *Contrib. Mineral. Petrol.* **98**, 257-276.

VILLENEUVE, M.E., ROSS, G.M., THÉRIAULT, R.J., MILES, W., PARRISH, R.R. & BROOME, J. (1993): Tectonic subdivision and U–Pb geochronology of the crystalline basement of the Alberta basin, western Canada. *Geol. Surv. Can., Bull.* **447**.

YARDLEY, B.W.D. (1989): *An Introduction to Metamorphic Petrology*. Longman, London, U.K.

*Received March 20, 1997, revised manuscript accepted August 20, 1997.*